JJMIE

Volume 13, Number 3, October. 2019
ISSN 1995-6665
Pages 191 - 196

Jordan Journal of Mechanical and Industrial Engineering

Unconfined Laminar Nanofluid Flow and Heat Transfer Around a Square Cylinder with an Angle of Incidence

Rafik Bouakkaz[a*], Yacine Khelili[a], Faouzi Salhi[b]

[a] *Military academy of Cherchell, Tipaza, Algeria.*
[b] *Département de Génie Mécanique, université Mouloud Mammeri Tizi ouzou*

Received 5 November. 2018

Abstract

A finite-volume method simulation is used to investigate two-dimensional unsteady flow of nanofluids and heat transfer characteristics past a square cylinder inclined with respect to the main flow in the laminar regime. The computations are carried out of nanoparticle volume fractions varying from 0 ≤ ≤ 5% for an inclination angle in the range 00≤ δ ≤ 450 at a Reynolds number of 100. The variation of stream line and isotherm patterns are presented for the above range of conditions. Also, it is noticed that the addition of nanoparticles enhances the heat transfer. Hence, the local Nusselt number is found to increase with increasing value of the concentration of nanoparticles for the fixed value of the inclination angle.

Keywords: Copper nanoparticles, heat transfer, square cylinder, inclination angle;

Nomenclature

L	side of the square cylinder	m
$\overline{Nu}$	average Nusselt number	
Nu_{local}	local Nusselt number	
Re	Reynolds number	
Pr	Prandtl number	
T_∞	free-surface temperature	k
U_∞	free-stream velocity	ms^{-1}
u	Stream-wise velocity	ms^{-1}
v	Cross-stream velocity	ms^{-1}

Greek symbols

ϕ	nanoparticle volume fractions	
δ	angle of incidence	^{0}
ϴ	non-dimensional temperature	
ν	kinematic viscosity	$m^2 s^{-1}$

1. Introduction

In recent years, studies about free convective fluid flow and heat transfer around square cylinder has been a subject of enormous attention for scientists due to its high applicability in many environmental situations or engineering developments such as, textile, thermal insulation, buildings, electronic equipments and chemical processing industries, etc. Despite the configuration being simple, the flow around a square cylinder involves a complex transport phenomenon because of a lot of factors, such as the effect of angle of incidence on the creation of lift force, evolution of streamline and temperature field, etc. This work is concerned with the characteristics of flow of Cu–water nanofluid and heat transfer past a square cylinder with varying values of angle of incidence in the unsteady laminar regime.

In literature, enough information is available presenting convective heat transfer characteristics around a square cylinder [1-5]. The effect of blockage ration on the fluid flow from a square cylinder at angle incidence of 0–45 and Re = 45–200 has been investigated by Sohankar et al. [6]. Subsequently, Sohankar et al. [7] studied numerically the characteristics of unsteady flow for the same configuration for Reynolds number (Re = 150–500) and a blockage ratio of 5.6%. Their results show a two-dimensional laminar shedding flow at Re= 150, and at Re = 200 the flow becomes three-dimensional. A well-organized study was also published by Robichaux et al [8]. In that paper, the onset of three-dimensionality in the wake of a square cylinder was analyzed by Floquet stability to show the different modes of 3-D instabilities. They establish that the 3-D disturbance first becomes unstable at a Reynolds number of about 161. Further, a parametric study was carried out by [9] with various values of angle of incidence and Re. They established critical Reynolds number for periodic vortex shedding at each angle of incidence. Recently, a direct numerical simulation was applied by Rastan [10] et al. to investigate three-dimensional unsteady flow characteristics around a finite wall-mounted square cylinder with an aspect ratio of 7 at a Reynolds number

* Corresponding author e-mail: r.bouakkaz@gmail.com

(Re) of 40-250. They found that the wake flow becomes turbulent at Re > 200. In past studies, the fluids used have a low value of thermal conductivity, which limits heat transfer. For this reason, there are several methods to improve the heat transfer characteristics, which consist in adding high conducting solid particles in the base fluid. The resulting fluid is called ‘‘nanofluid’’ [11–12]. Furthermore, [13] have studied the momentum and forced convection heat transfer for a laminar and steady free stream flow of nanofluids past an isolated square. Various nanofluids consisting of Al_2O_3 and CuO with base fluids of water and a 60:40 (by mass) ethylene glycol and water mixture were selected to estimate their superiority over conventional fluids. They established that for any given particle diameter, there is an optimum value of particle concentration that results in the highest heat transfer coefficient. The fluid flow and heat transfer around a square cylinder utilizing Al_2O_3–H_2O nanofluid over low Reynolds numbers varied within the range of 1 to 40 and the volume fraction of nanoparticles (ϕ) is varied within the range of $0 < \phi < 0.05$ was also investigated by [14]. They found that increasing the nanoparticles volume fractions augments the drag coefficient. Moreover, Pressure coefficient increases by increasing the solid volume fraction for sides where pressure gradient is inverse, but for sides where the pressure gradient is favourable the pressure coefficient decreases. Recently, Rajendra et al. [15] have carried out a meticulous study on the forced convective heat transfer from an unconfined heated square cylinder utilizing nanofluids with multiphase modelling approach for different Reynolds number (10-40) and volume fractions of Al_2O_3 particles (0-5%) in water. The results indicated that the effect of Nano layer thickness and nanoparticle diameter on the overall heat transfer rate can be studied. So, the aim of the current study is to investigate numerically by using a finite volume method based on SIMPLE algorithm the laminar flow of nanofluid and heat transfer characteristics for an inclination angle in the range $0^0 \le \delta \le 45^0$ under the particle volumetric concentrations ranging from 0% to 5% at Reynolds numbers (Re =100).

2. Governing equations and boundary conditions

The governing partial differential equations here are the Navier-Stokes and energy equations in two dimensions the incompressible nanofluid flow around a square cylinder are given blow:

$$\frac{\partial U}{\partial X}+\frac{\partial V}{\partial Y}=0 \tag{1}$$

$$\frac{\partial U}{\partial \tau}+U\frac{\partial U}{\partial X}+V\frac{\partial U}{\partial Y}=-\frac{\partial P}{\partial X}+\frac{1}{\mathrm{Re}}\frac{\nu_{nf}}{\nu_f}\left(\frac{\partial^2 U}{\partial X^2}+\frac{\partial^2 U}{\partial Y^2}\right) \tag{2}$$

$$\frac{\partial V}{\partial \tau}+U\frac{\partial V}{\partial X}+V\frac{\partial V}{\partial Y}=-\frac{\partial P}{\partial Y}+\frac{1}{\mathrm{Re}}\frac{\nu_{nf}}{\nu_f}\left(\frac{\partial^2 V}{\partial X^2}+\frac{\partial^2 V}{\partial Y^2}\right) \tag{3}$$

$$\frac{\partial \theta}{\partial \tau}+U\frac{\partial \theta}{\partial X}+V\frac{\partial \theta}{\partial Y}=\frac{1}{\mathrm{Re}\,\mathrm{Pr}}\frac{\alpha_{nf}}{\alpha_f}\left(\frac{\partial^2 \theta}{\partial X^2}+\frac{\partial^2 \theta}{\partial Y^2}\right) \tag{4}$$

Where:

$$U=\frac{u}{U_\infty},V=\frac{v}{U_\infty},X=\frac{x}{L},Y=\frac{y}{L},\tau=\frac{tU_\infty}{L},$$

$$P=\frac{p}{\rho U_\infty^2},\mathrm{Pr}=\frac{\nu_f}{\alpha_f},\mathrm{Re}=\frac{U_\infty L}{\nu_f},\theta=\frac{T-T_\infty}{T_w-T_\infty}$$

Where U and V are the velocity components along X and Y axes, T denotes the temperature, P is the pressure, ρ is the density, μ the dynamic viscosity. The subscript *nf* stands for nanofluid, the subscript *f* stands for base fluid and the subscript s stands for solid nanoparticles. The thermophysical properties taken from [11], for the base fluid and copper oxide (at 300 K) are shown in Table 1.

Table 1. Thermo-physical properties of the base fluid and the Cu nanoparticles

Property	Water	Copper
$C_p\left(JKg^{-1}K^{-1}\right)$	4179	385
$\rho\left(Kgm^{-3}\right)$	997.1	8.933
$k\left(Wm^{-1}K^{-1}\right)$	0.613	401

3. Boundary conditions

The dimensionless boundary conditions for the flow across a square cylinder surrounded by Cu-water nanofluid can be written as (Figure 1): The left-hand section, the Dirichlet-type boundary condition for the Cartesian velocity components is assumed.

$$U=1,\ V=0 \text{ and } \theta=0 \tag{5}$$

The right-hand, the diffusion flux in the direction normal to the exit surface is zero for all variables,

$$\partial U/\partial X=\partial V/\partial X=\partial \theta/\partial X=0 \tag{6}$$

On the straight horizontal segments (slip boundary), a zero normal velocity and a zero normal gradient of all variables are prescribed:

$$\partial U/\partial Y=\partial V/\partial Y=\partial \theta/\partial Y=0 \tag{7}$$

Finally, the dimensionless peripheral or tangential velocity is prescribed on the surface of the cylinder along with a no-slip boundary condition

$$U=0,\ V=0 \text{ and } \theta=1 \tag{8}$$

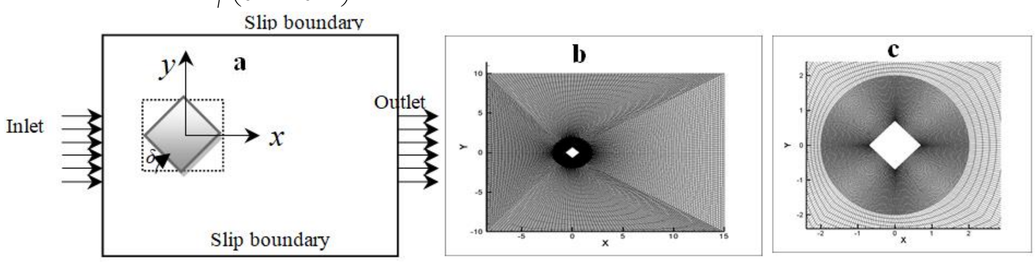

Figure 1. (a) Schematic of the unconfined flow and heat transfer around a square cylinder. (b) Grid structure. (c) Close-up view in the vicinity of the square cylinder.

The effective density, the thermal diffusivity, the heat capacitance, the effective dynamic viscosity and the effective thermal conductivity of the nanofluid are calculated using the following expressions:

$$\rho_{nf} = (1-\phi)\rho_{bf} + \phi\rho_s \tag{9}$$

$$(\rho C_p)_{nf} = (1-\phi)(\rho C_p)_{bf} + \phi(\rho C_p)_s \tag{10}$$

$$\alpha_{nf} = k_{nf} / (\rho C_p)_{nf} \tag{11}$$

$$\mu_{nf} = \frac{\mu_{bf}}{(1-\phi)^{2.5}} \tag{12}$$

$$k_{nf} = k_{bf}\left[\frac{(k_s + 2k_{bf}) - 2\phi(k_{bf} - k_s)}{(k_s + 2k_{bf}) + \phi(k_{bf} - k_s)}\right] \tag{13}$$

Where φ is the solid volume fraction and given as:

$$\phi = \frac{\text{Volume of nanopartides}}{\text{Total volume of solution}} \tag{14}$$

4. Force Coefficient

The relevant parameters computed from the velocity and pressure fields are the drag coefficient, which represent dimensionless expressions of the forces that the fluid produces on the circular cylinder. Defined as:

$$C_D = \frac{\mathrm{D}}{\rho U_\infty^2 L} \tag{15}$$

where D is the drag force.

5. Results and discussion

5.1. Numerical details

The unsteady, laminar, segregated solver was employed here to solve the incompressible flow on the collocated grid arrangement. Semi implicit method for the pressure linked equations (SIMPLE) was used to solve Navier-Stokes and energy equations for above noted boundary conditions. Second order upwind scheme is used to discretize the convective terms of momentum equations, whereas the diffusive terms are discretized by central difference method. A convergence criterion of 10^{-8} is used for continuity, and x-y components of momentum equations. While, for energy equation the criteria of convergence were 10^{-10}. The numerical resolution was determined by a grid refinement study to ensure grid independency. The mesh used for all the two-dimensional computations consisted of 39200 quadrilateral cells and 39480 nodes. The grid is divided into two separate zones, and uniform as well as no uniform grid distributions are employed. The grid distribution was made uniform with a constant cell size, of 0.02, inside a region around the cylinder that extended 4 units to capture wake–wall interactions adequately. Then, a grid of much bigger size is clustered around the cylinder over the distance indicated above.

5.2. Comparison with other results

Table 2 compares the mean Nusselt number and drag coefficients computed here with results obtained from the literature. We have noted that the Nusselt number and drag coefficient values are in superb agreement with numerical data reported by other researchers.

Table 2. Comparison of Nu number and drag coefficient computed in the present study with literature data (Pr = 0.7)

	Re = 20		Re = 40		Re = 100	
	Nu	CD	Nu	CD	Nu	CD
Present study	2.07	2.43	2.71	1.81	4.07	1.51
Paliwali et al. [16]	2.07	-	2.71	1.98	-	-
Sharma and Eswaran [3]	2.05	2.35	2.71	1.75	-	-
Etminan-Farooji [13]	2.07	2.43	2.72	1.83	-	-
Sahu et al. [5]	-	-	-	-	4.03	1.49
Prasenjit [17]	-	-	-	-	3.84	1.53

5.3. Flow patter

Within the full range of possible incidences, this study indicated two different flow patternsnamely, Main separation, and Vortex creation, as illustrated in figure 2. These flow patterns are summarized below.

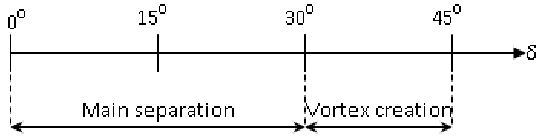

Figure 2. Flow patterns past a square cylinder with an angle of incidence at Re=100.

5.4. Main separation

Figure 3 shows the case of instantaneous streamlines past a square cylinder at δ =0°. In the Main separation pattern, main vortices of opposite sign roll up in an alternating manner as mentioned in Perry et al. [16] and instant 'alleyways' of fluid enter the cavity as well as an alleyway flow indicated by the arrows between. However, once the vortex-shedding process begins, this so-called 'closed' cavity becomes open, and instantaneous 'alleyways' of fluid are created which penetrate the cavity.

5.5. Vortex creation

The vortex merging pattern is characterized by creation and merging of two small vortices which are originally produced by separation and subsequent reattachment of the alleyway flow at two neigh boring edges of the square cylinder. Clearly, in figure 4, the vortices A and B are generated due to separation and reattachment of the alleyway flow. The two vortices are merged into a big one, C Figure 4b. The vortex C is shed into the wake H in Figure 4c, and small vortices D and E are produced by the opposite alleyway flow, Figure 4c. Vortices D and E are merged into F, Figure 4d. In most cases of vortex merging pattern, an alleyway flow exhibits the characteristic feature of the Vortex creation pattern, generation and subsequent merging of two small vortices, in an alternating manner with a downwash or an up-wash flow in the alleyway like in figure 4.

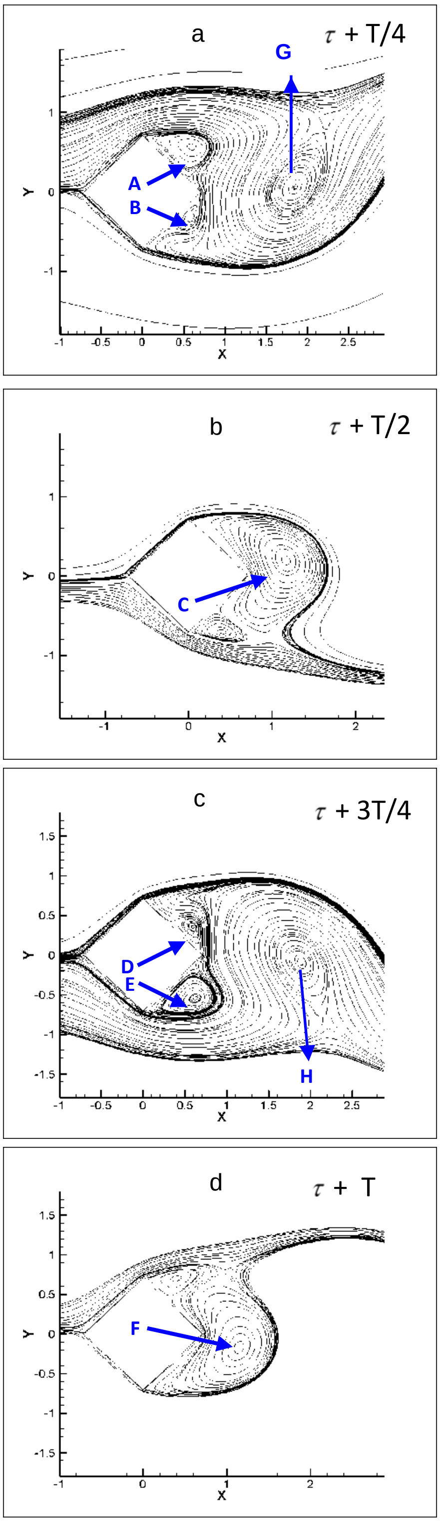

Figure 4. Instantaneous streamlines (base fluid) for Vortex creation, where T is one period of vortex shedding**.**

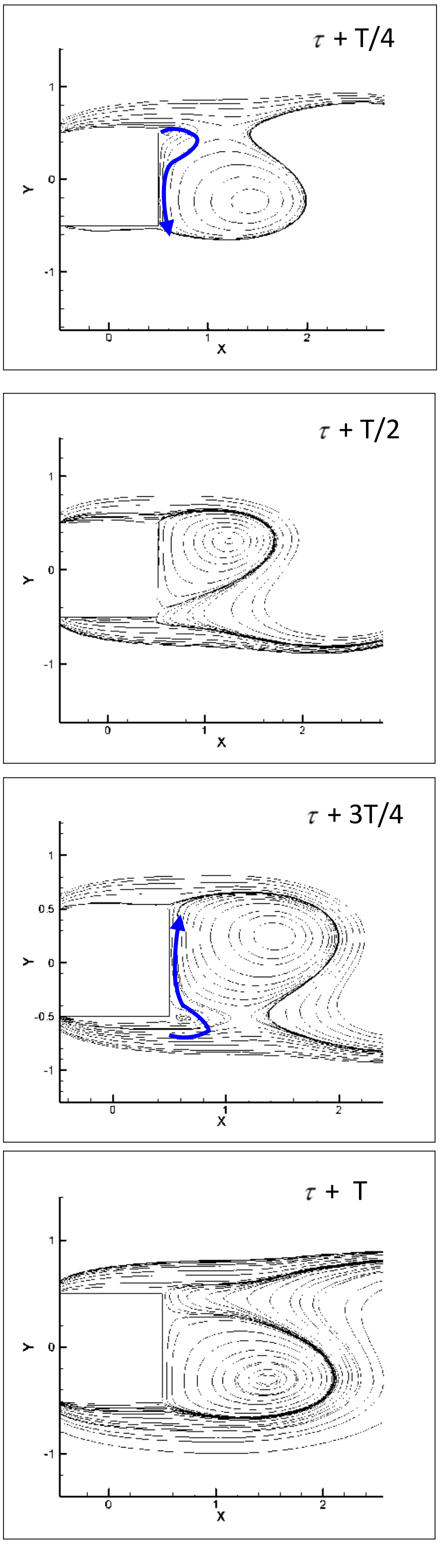

Figure 3. Color online Instantaneous streamlines (base fluid) for Main separation pattern, where T is one period of vortex shedding.

5.6. Isotherm patterns

The isotherms profiles around the cylinder for Reynolds number of 100 at $\delta=15^0$ are compared between base fluid and nanofluid (ϕ =0.05) in figure 5. Clearly, the temperature distribution contours for base fluid are overlaid with that for nanofluid. This can be explained as the addition of solid particles to the base fluid increases the Reynolds number of nanofluid. Hence, a higher capacity of transferring the heat from the cylinder. It is obvious from Figure 4 that the isotherms have maximum density close to the front surface of the cylinder (AB); this indicates high values of the local Nusselt number near the front stagnation point on the front surface as compared to other points on the cylinder surface.

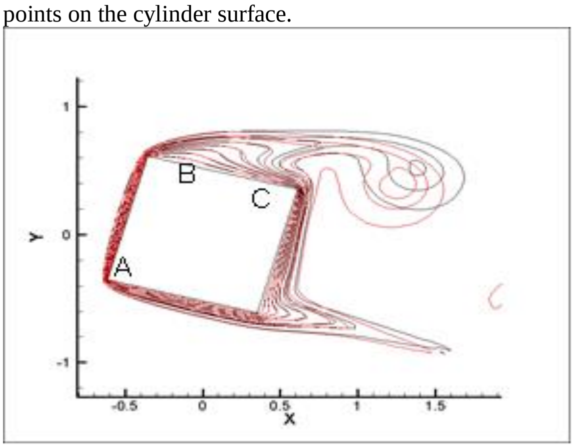

Figure 5. Temperature contours for the flow around the square cylinder (red line refers to base fluid and black line refers to nanofluid with solid volume fraction 0.05) at $\delta=15^0$

5.7. Local Nusselt number

The local Nusselt number is calculated to evaluate the warmth transmission behaviour around the cylinder and given as:

$$Nu_{local} = \frac{h_{local}.D}{K_f} = -\left(\frac{k_{nf}}{k_{bf}}\right)\frac{\partial \theta}{\partial n} \quad (16)$$

Figure 6 shows the variation of local Nusselt number (Nu) on the surface of the square cylinder with increase for various volume fraction ϕ at $\delta=15^0$. When the solid concentration increases, the thermal conductivity improves and consequently the local Nusselt number. Additionally, the thermal boundary layer is decreased by any increase in solid volume fraction. Therefore, the local Nusselt number is enhanced by any increasing in solid volume fraction (ϕ). Further, these plots also show that the Nusselt number along the left half of the face (AB) of the cylinder increases, it has a maximum at the corner of the square cylinder (B). On the other hand, a value for the inclination angle of $\delta=45^0$ is found for which the local Nusselt number is highest along the left half of the face (BC) as seen in Figure 7.

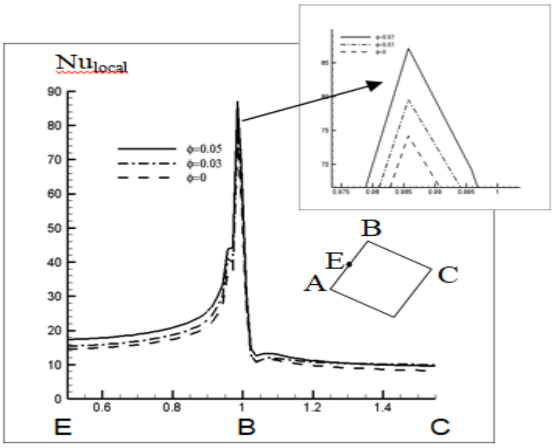

Figure 6. Local Nusselt number variation for $\delta=15^0$ at various solid volume fractions.

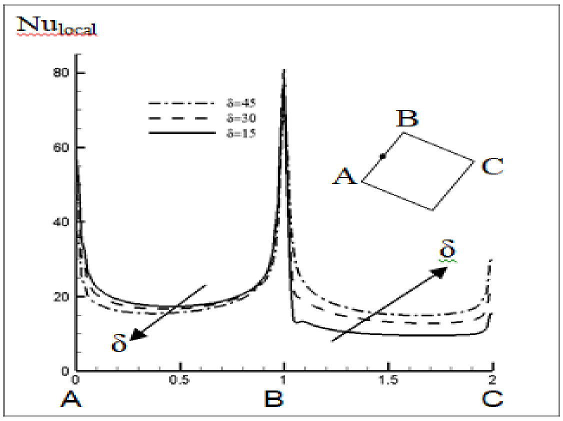

Figure 7. Local Nusselt number variation for ϕ =0.05 at various angle of incidence.

5.8. Averaged Nusselt number

Surface averaged Nusselt number of fully developed thermal boundary layer is defined as:

$$\overline{\mathrm{Nu}} = \frac{1}{S}\int_s Nuds \quad (17)$$

The average Nusselt number variation is presented in figure 8 for the solid volume fraction varying from 0 to 0.05 at different angle of incidence. This figure indicates that the averaged Nusselt number increases with increasing solid volume fraction of nanoparticles (ϕ) of the fixed value of the angle of incidence. This can be explained as when ϕ number increases the inertia of flow increases thus increasing the heat transfer. Also, the average Nusselt number is highest at δ =45°.

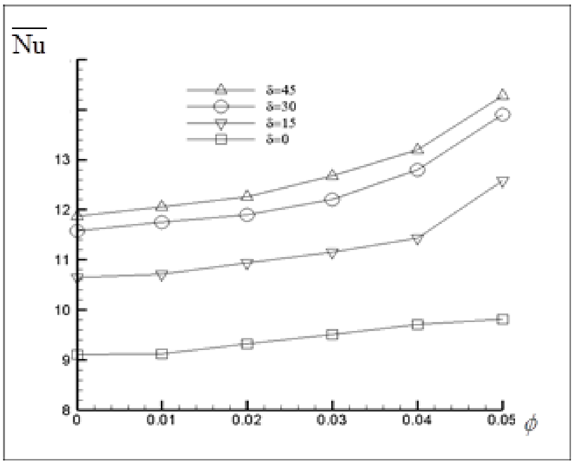

Figure 8. Variation of average Nusselt number at various solid volume fractions for varying values of angle of incidence.

6. Conclusions

The present study focuses on the unconfined laminar flow of nanofluid and heat transfer characteristics around a square cylinder under the influence of various angle of incidence in the unsteady regime. The illustrative streamline shows two different flow patterns, namely, Main separation, and Vortex creation. Further, the temperature distribution contours for base fluid are overlaid with that for nanofluid. This can be explained as the addition of solid particles to the base fluid increases the Reynolds number of nanofluid. Hence, a higher capacity of transferring the heat from the cylinder. On the other hand, the isotherms have maximum density close to the front surface of the cylinder; this indicates high values of the local Nusselt number near the front stagnation point on the front surface as compared to other points on the cylinder surface. Finally, it was showed that the average Nusselt numbers were enhanced by adding nanoparticles to base fluid for various angle of incidence. Moreover, the average Nusselt number is highest at δ =45°.

References

[1] M. Sarioglu, Y. E. Akansu, and T. Yavuz, “Control of flow around square cylinders at incidence by using a rod”, AIAA J (2005) 43, 1419

[2] T. Igarashi, “Characteristics of the flow around a square prism,” Bull. JSME 1984, 27, 1858

[3] A. Sharma, V. Eswaran, “Heat and fluid flow across a square cylinder in the two-dimensional laminar flow regime”, Numer. Heat Transfer A (2004) 45, 3, 247– 269.

[4] A.K. Dhiman, R.P. Chhabra, V. Eswaran, “Flow and heat transfer across a confined square cylinder in the steady flow regime: effect of Peclet number”, Int. J. Heat Mass Transfer (2006) Part A, 49: 717–731.

[5] A.K. Sahu, R.P. Chhabra, V. Eswaran, “Effects of Reynolds and Prandtl numbers on heat transfer from a square cylinder in the unsteady flow regime”, Int. J. Heat Mass Transfer (2009) 52(3), 839–850.

[6] A. Sohankar, C. Norberg, L. Davidson, “Low-Reynolds-number flow around a square cylinder at incidence: study of blockage, onset of vortex shedding and outlet boundary condition”, Int. J. Numer. Methods Fluids (1998) 26, 39

[7] A. Sohankar, C. Norberg, L. Davidson, “ Numerical simulation of unsteady fow around a square two-dimensional cylinder”,Proceedings of the 12th Australasian Fluid Mechanics Conference, Sydney,Australia (1995) pp. 517–520.

[8] J. Robichaux, S. Balachandar, and S. P. Vanka, “Three-dimensional
Floquet instability of the wake of square cylinder,” Phys. Fluids (1999) 11, 560

[9] Dong-Hyeog Yoon, Kyung-Soo Yang,a and Choon-Bum Choi , “Flow past a square cylinder with an angle of incidence”, PHYSICS OF FLUIDS (2010) 22, 043603

[10] M. R. Rastan, A. Sohankar, and Md. Mahbub Alam , “Low-Reynolds-number flow around a wall-mounted square cylinder: Flow structures and onset of vortex shedding ”,Physics of Fluids (2017) 29, 103601.

[11] R.Bouakkaz et al., “Unconfined laminar nanofluid flow and heat transfer around a rotating circular cylinder in the steady regime ”, archives of thermodynamics (2017) 38, No. 2, 3–20.

[12] H.C. Brinkman, “The viscosity of concentrated suspensions and solutions”, The journal of Chemical Physics 20 (1952) 571–581.

[13] V.E. Farooji., E.E.Bajestan, H.Niazmand, S.Wongwises, “Unconfined laminar nanofluid flow and heat transfer around a square cylinder”, Int. J. Heat Mass Tran. 2012,55, 5-6, 1475–1485.

[14] M.S. Valipour, R Masoodi, S. Rashidi, M. Bovand, M. Mirhosseini. “A numerical study on convection around a square cylinder using AL2O3-H2O nanofluid”, Therm. Sci. (2014) 18, 4, 1305–1314.

[15] S. Rajpoot Rajendra, S. Dhinakaran, “Study of heat transfer from a square cylinder utilizing nanofluids with multiphase modeling approach Materials Today”, Proceedings (2017) 4 ,10069–10073

[16] A. E. Perry, M. S. Chong, and T. T. Lim, “The vortex-shedding process behind two-dimensional bluff bodies,” J. Fluid Mech (1982.)116, 77

[17] Dey Prasenjit and Das Ajoy kumar , “Analysis of Fluid Flow and Heat Transfer Characteristics Over a Square Cylinder: Effect of Corner Radius and Nanofluid Volume Fraction ,” Arab J Sci Eng (2015) DOI 10.1007/s13369-016-2276-2